Journal of GeoEngineering, Vol. 14, No. 4, pp. 247-257, December 2019
http://dx.doi.org/10.6310/jog.201912_14(4).4

EXPERIMENTAL STUDY ON SHAKEDOWN COMPRESSION OF SATURATED GRANULAR SOILS DUE TO PORE PRESSURE VARIATION

Wen-Jong Chang [1*] and Shih-Hsun Chou [2]

ABSTRACT

Field data revealed that compression in aquifer layers is the major source of ground subsidence and that compression of saturated granular soils due to fluctuations in pore pressure is important in this context. To investigate the mechanism of granular soil compression due to repeated pore pressure variations, a modified Rowe cell is developed to mimic the stress conditions in the field. The shakedown theorem is extended to saturated, granular soils under K_o condition. Remolded sand specimens with different mica contents are prepared to study the shakedown behaviors. Experimental results show that saturated granular soils under K_o condition will always be below the plastic shakedown limit, and shakedown responses are affected by the pore pressure amplitude, soil composition, and initial state. Comparisons of monotonic and shakedown compression reveal that the shakedown compression is at least as significant as the monotonic compression component, and clearly show that the shakedown effect should be included in ground subsidence analysis.

Key words: Sands, compressibility, shakedown, K_o consolidation.

1. INTRODUCTION

Significant excess subsidence from excessive groundwater pumping or climate change is a serious problem in many alluvial deposits around the world and it threatens the operation of infrastructures, induces prolonged flooding, and causes sea water intrusion. Current approaches to land subsidence modeling are generally based on calculating the maximum changes in vertical effective stress from the reduction in pore pressure, and then using either Terzaghi (1925) one-dimensional consolidation (Hill *et al.* 2000) or Biot (1941) three-dimensional consolidation theory to estimate the land subsidence (Burbey 2006). In other words, aquitards and interbeds consisting of fine-grained silts and clays are the main contributors to ground subsidence due to the higher compressibility of cohesive soils than those of granular ones.

However, field monitoring data in central western Taiwan show the significance of compression in thick aquifer layers. Hung *et al.* (2012) reported that the compression of the top three aquifer layers, which mainly consist of fine to coarse sand with occasional layers of gravel, contributed 83% of the ground subsidence during the period of 1997 to 2010. Specifically, the accumulated vertical compression observed in the confined aquifer layer at a depth from 52 to 153 m was up to 63.4 cm under the maximum pore pressure variation of 13 m in this period. Additionally, the temporal variations of the ground water level can be divided into the long-term trend and short-term oscillations. The temporal inconsistency between the induced compression and the long-term pore pressure trend in the aquifer layer implies that the concept of conventional, monotonic consolidation theory is insufficient for subsidence prediction in granular soils (Chang *et al.* 2017).

To take into account the compression of granular soils due to ground water fluctuation, Chang *et al.* (2017) introduce the shakedown theorem, which has been widely used in pavement engineering, to describe the permanent deformation of unbounded granular layers subjected to repeated loading to interpret the accumulation of compression of granular soils under repeated loading. In Chang *et al.* (2017) paper, the K_o consolidation tests were performed in a triaxial cell and the accurate control of lateral deformation is crucial because of the small normal strain in granular soil specimens. To ascertain the significance of ground subsidence from the compression of granular soils due to the short-term fluctuation of ground water levels, a series of element tests that mimic the in situ fluctuated stress paths were performed in this study using a newly developed K_o consolidation/compression system. A modified Rowe cell (Rowe and Barden 1966), which is capable of controlling the drainage and back pressure conditions, is loaded with a closed-loop, servo-controlled loading frame. Specimens made of quartz sand mixed with mica were subjected to slow, sinusoidal variations of pore water pressure while maintaining a constant total vertical stress and K_o conditions. The effects of shakedown compression by repeated pore pressure variations on saturated sands are presented in this study.

2. COMPRESSIBILITY OF GRANULAR SOILS

2.1 Studies of Compressibility in Granular Soils

Granular soils are highly nonlinear, anisotropic, and effective stress dependent materials with complex deformation

Manuscript received March 20, 2019; revised July 8, 2019; accepted July 15, 2019.
[1*] Professor (corresponding author), Department of Civil Engineering, National Cheng Kung University, Tainan, Taiwan 70101, R.O.C. (e-mail: wjchang@mail.ncku.edu.tw).
[2] Graduate Research Assistant, Department of Civil Engineering, National Cheng Kung University, Tainan, Taiwan 70101, R.O.C.

characteristics. Chuhan *et al.* (2003) concluded that the porosity at any given effective stress level is highly dependent on the grain-size distribution, grain shape, and mineralogy, and significant particle crushing can occur at vertical stresses of 2 to 8 MPa. The plastic strain in confined compression is mainly from particle sliding and rolling at a low stress level, and particle crushing at medium to large stress conditions (Nakata *et al.* 2001; Pestana and Whittle 1995). Based on previous studies on the mechanism of sand compression and field stress state, the subsidence of an aquifer layer from groundwater pumping is likely due to granular particle rearrangement and a reduction in porosity.

In the field, a soil element is subjected to K_o condition, in which the lateral strain is prohibited when subjected to variations of vertical stress. Several testing procedures and apparatus have been developed to determine the compressibility or consolidation characteristics of soils in K_o conditions, including oedometer test (Casagrande 1960), constant rate of strain consolidation (CRS) test (Wissa *et al.* 1971; Lee 1981), and Rowe cell (Rowe and Barden 1966). The major differences are the stress application process, excess pore pressure measurement, and drainage boundary control.

There have been few studies on the compressibility of granular soils from cyclic loadings. Lambe and Whitman (1969) conducted a theoretical study of the ideal packing of elastic spheres to describe the effects of cyclic loading on stress-strain curves during confined compression. Their study concluded that a small amount of permanent strain accumulated during the first 10 to 50 cycles of loading for particles without crushing. After this state, a stable hysteretic loop without further accumulation of permanent strain is achieved. The critical stress needed to induce permanent strain is generally small and increases with the previous loading level and rate. Leshchinsky and Rawlings (1988) used a pneumatic servo-controlled triaxial system to study the effects of stress path on the permanent deformation of dry sand and found a linear relationship between the permanent axial strain and the logarithm of the number of loading cycles. These studies revealed that characteristics of granular compressibility from repeated loadings are different from those of monotonic loadings.

2.2 Shakedown Theorem

The shakedown theorem (Melan 1938; Koiter 1960) has been used to describe the behavior of elasto-plastic materials under cyclic loading (Sharp and Booker 1984; Werkmeister *et al.* 2004). In the shakedown theorem, the material response under cyclic loadings is divided into four stages, which are elastic, elastic shakedown, plastic shakedown, and incremental collapse or ratcheting. The loading limits that separate the four stages are elastic limit, elastic shakedown limit, and plastic shakedown limit. Shakedown stages occur when the applied load magnitude is greater than the elastic limit but smaller than a critical limit at which incremental collapse is initiated. In the shakedown stages, the material deforms plastically in each loading cycle and the permanent deformation rate decreases rapidly to zero or a small value, which in turn results in an asymptotic or linear relationship in permanent strain-loading cycle curves. In other words, the accumulation of plastic deformation ceases or slowly increases after a finite number of loading cycles. If the steady response is linearly elastic, then the stage is called elastic shakedown. Plastic shakedown occurs when the load magnitude is greater than the elastic shakedown limit but less than the plastic shakedown limit. In this stage, the material achieves a resilient or steady response with a nonlinear, hysteretic stress-strain relationship. The terms plastic shakedown and plastic creep are for zero and small deformation rates, respectively. When the material reaches the resilient condition, the material is said to be "shaken down". The ratcheting stage indicates that plastic strains accumulate rapidly with failure occurring in a short time.

Shakedown strain models have been proposed to relate the permanent strain with the number of load repetitions in logarithmic or power forms (Barksdale *et al.* 1972). Barksdale *et al.* (1972) proposed that the permanent strain (ε_p) can be described as:

$$\varepsilon_p = a + b\log(N) \tag{1}$$

where N is the number of loading cycles and a, b are regression parameters. Previous studies on shakedown responses of granular materials were mainly on unsaturated, shallow, moving surface loaded, and laterally free stress soils, such as the unbounded granular layer in a pavement system. Chang *et al.* (2017) first studied the shakedown behavior of saturated sand with K_o-triaxial consolidation system and reveled that saturated, granular soils show typical shakedown behaviors in drained condition. Limited by the accuracy of strain measurement and control of lateral strain, only a few quantitative details are presented.

In the case of the ground subsidence of aquifer layers owing to fluctuations of pore water pressure, granular soil layers were within the shakedown stage with plastic strain accumulation before they achieved a steady response. In the shakedown framework, the aquifer soil is likely to undergo the plastic shakedown condition, in which a significant portion of settlement induced from the accumulation of plastic strain during cyclic loading and the settlement could cease after a finite number of cycles. This type of response is also called cyclic strain hardening and can be expressed by adding a residual stress field in the yielding criteria (Yu 2005). Comparisons between the shakedown and monotonic compressions of saturated granular soils are performed in this study. The significant difference in compressibility between shakedown and monotonic compressions provides a basis for interpreting and predicting ground subsidence owing to pore pressure fluctuations.

2.3 Shakedown State in Ground Subsidence

In Melan's lower-bound shakedown theorem, shakedown occurs if any self-equilibrated residual stress field (σ_{ij}^r) combined with the elastic stress field (σ_{ij}^e) from applied loads does not violate the yield condition anywhere. This can be expressed as:

$$f(\lambda\sigma_{ij}^e + \sigma_{ij}^r) \le 0 \tag{2}$$

where λ is a dimensionless scale parameter. Yu (2005) presented the three-dimensional analytical solution for the shakedown of Mohr-Coulomb materials under a moving Hertz load. Adopting the procedure and assuming both elastic and residual stresses following the K_o stress condition, the stress components under one-dimensional K_o compression can be expressed as:

$$\sigma'_v = \lambda\sigma_v^e + \sigma_v^r \tag{3a}$$

$$\sigma'_r = \lambda(K_o\sigma_v^e) + (K_o\sigma_v^r) \tag{3b}$$

$$\tau_{vr}^e = \tau_{vr}^r = 0 \tag{3c}$$

where σ'_v and σ'_r are vertical and lateral effective stresses, τ_{vr} is

the shear stress on the vertical plane, and superscripts *e* and *r* represent the elastic and residual effective stress components, respectively. Adopting the Mohr-Coulomb yielding criteria for granular soils (*i.e.*, $c' = 0$), the necessary condition for a shakedown to occur is that the stress field defined by Eqs. 3(a) ~ 3(c) satisfies the following inequality:

$$(\lambda\sigma_v^e + \sigma_v^r)\left[(1 - K_o) - \sin\phi'(1 + K_o)\right] \le 0 \tag{4}$$

where ϕ' is the effective friction angle of soil, and the vertical and lateral stress components are effective ones. According to Jaky (1944), the K_o value can be approximated by $(1 - \sin\phi')$, resulting in a negative value within the bracket. In order to satisfy the shakedown condition of Eq. (4), the following must be met:

$$\lambda \le \frac{-\sigma_v^r}{\sigma_v^e} \tag{5}$$

A negative λ value represents tensional vertical stress. A plastic shakedown limit only occurs in large tensional vertical stress, which is invalid due to the low tension strength of soils. Therefore, K_o compression always occurs below the plastic shakedown limit, and the permanent compression will eventually cease or slowly linearly increase when subjected to fluctuations in pore pressure.

3. TESTING SYSTEM

3.1 State of Stress and Stress Path

In the field, the subsurface soil element is subjected to a constant total vertical stress and maintained K_o condition throughout the process of pore pressure fluctuations due to pumping and seasonal water table variations. To systematically study the shakedown compressibility of aquifer soils subjected to repeated loadings, sinusoidal pore pressure variations with a constant amplitude were applied to a saturated soil element under a constant total vertical stress and K_o condition. The stress path is referred to as the back-pressure-controlled compression (BPCC) approach by Chang *et al.* (2017). The BPCC stress path can reduce the stress difference from K_o variations with pre-stress histories to a greater degree than the loading paths with constant pore pressure and varying total vertical stress.

To fit the plastic shakedown condition, a constant amplitude of pore pressure variation is cyclically applied on the saturated soil specimen until the increment of induced permanent vertical displacement approaches zero or a small constant value. To reduce the effort and inconsistencies involved in sample preparation, a multi-stage testing procedure is adopted. After the completion of consolidation to static vertical effective stress, small pore pressure amplitude is cyclically applied until a steady or resilient state is observed. The pore pressure amplitude is then increased and the process is repeated.

3.2 System Overview

To mimic the aforementioned stress paths, two types of compression tests are available: the K_o triaxial consolidation and Rowe cell. The Casagrande oedometer is excluded because of lacking pore pressure control. Menzies *et al.* (1978) developed an automatic K_o triaxial consolidation system, which integrated a lateral strain caliper in a conventional triaxial cell. The concerns with this technique include being less representative of the average radial deformation in non-uniform deformation, and errors from membrane penetration. Furthermore, the triaxial K_o consolidation is limited to a pressure range of less than 1 MPa due to the conventional pneumatic pressure supply and electronic waterproof capacity.

To ensure the K_o condition during the loading process and increase the stress level, the design concept of the Rowe cell was adopted to perform high pressure K_o compression subjected to pore pressure variations using the BPCC approach. Because the new system is for ground subsidence simulation in high stress conditions, it is termed the HPK_o simulator and shown in Fig. 1(a). The HPK_o simulator consists of three major subsystems: the K_o compression cell, stress control system, and data acquisition (DAQ). Details of the hardware and control method are presented in the following sections, as are the results for granular soils mixed with mica. Additionally, the shakedown characteristics of saturated granular soils are shown for sand with and without mica content.

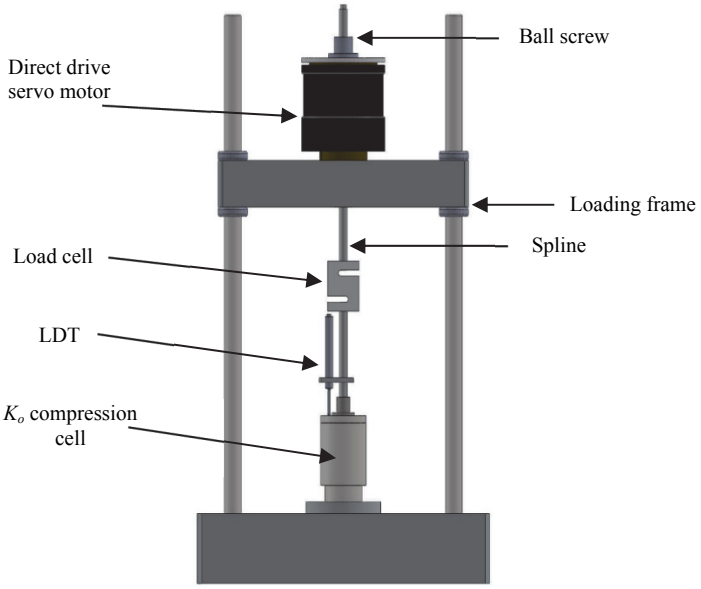

(a) Schematic of HPK_o system

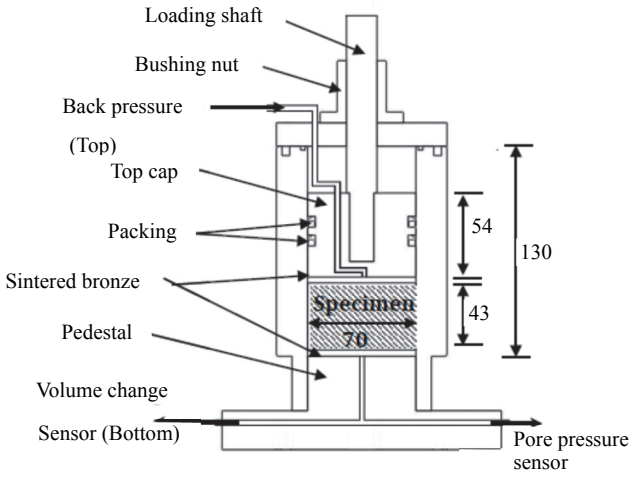

(b) High pressure K_o compression cell (unit: mm)

Fig. 1 Details of HPK_o simulator

3.3 K_o Compression Cell

The HPK_o simulator adopted the concept by Rowe and Barden (1966) to fully control the drainage and back pressure. Details of the K_o compression cell are shown in Fig. 1(b). Most of the components of the cell are made of stainless steel to provide enough rigidity and be resistant to corrosion. A cylindrical cell with an inner diameter of 70 mm is machined to be tightly housed on a pedestal. The inner wall is coated with thin Teflon to reduce the side friction. The bottom drainage paths have an outlet at the center of the pedestal top and are connected to a pore pressure transducer and back pressure regulator on the pedestal. The top cap is also made of stainless steel, with top drainage at the center of this. Sintered bronze plates with a thickness of 5 mm are used on both the top and bottom surfaces of the specimen. The loading shaft is bolted at the center of top cap and guided by a linear bushing nut. The system is designed to function as a rigid plate applied on the top of the specimen. A computer-based 24-bit data acquisition system is integrated to acquire data and provide feedback signals of the axial actuator and pressure regulators for stress control.

In the original Rowe cell, a convoluted rubber jack was used to provide the sealed condition and reduce the side friction during loading. However, the gap between the cell wall and convoluted diaphragm raises concerns with regard to volume measurement. Additionally, the applicable pressure limit of the rubber jack restricts the applicable stress level. To solve these issues, a low-friction, spring energized packing is used on the circumference of the rigid top cap to provide a sealed condition while allowing two-way acting under small and relatively constant side friction. The back pressure assists the packing spring in creating a leak-tight seal between the sealing lips and the mating metal parts. Teflon sealing lips are used to contact with the Teflon coated inner wall to reduce the side friction. The measured side friction is about 1 N and almost constant for a back pressure level up to 3 MPa. This value is used to compensate for the applied vertical loads.

The back pressure is applied from the top drainage while the pore pressure and volume change are measured at the center of the pedestal. This setup ensures the full equilibrium of the pore pressure within the specimen because it measures the longest drainage path for one-way drainage. The volume change is measured by an automatic volume change apparatus with an accuracy of 0.01 cm^3. An external linear displacement transducer (LDT) with a resolution of 0.001 mm is clamped on the loading rod to measure the vertical displacement of the specimen. A comparison between the volume changes of a saturated specimen from the LDT reading and volume change apparatus shows that the error is below the resolution of the volume change apparatus up to a vertical stress of 2.5 MPa, due to the high rigidity of the shaft, rigid top cap, energized seals, and well-aligned linear bushing nut.

3.4 Stress Control System

In order to adopt the BPCC method in ground subsidence simulation, the total vertical stress and pore pressure must be continuously adjusted to meet the stress conditions. Following the design by Huang *et al.* (1994), an electromagnetic actuator, consisting of a direct-drive (DD) servo motor, high precision ball screw, and spline shaft, is used to provide servo vertical stress control. The high torque capacity of the motor reduces the instability of the closed loop control. The combination of the ball screw and spline shaft converts the rotation motion to the high precision axial stroke. A new control concept is developed to unify the different layouts of stress- and strain-controlled into the same hardware configuration.

The DD motor, which is a brushless step motor with an embedded encoder for servo control, provides a rotation accuracy of 0.0125 degrees, peak torque of 110 N-m, axial compression force 40 kN, and axial tension force 20 kN. In the HPK_o simulator, the motor is divided into 614,400 steps per revolution. A zero-backslash ball screw with a lead (linear displacement per revolution) of 5 mm enables a linear motion accuracy of 3.1 μm, with an updating frequency of over 100 Hz. To take advantage of the high precision feature, the motor is setup for position control with a feedback signal from various sensors. The stress-controlled condition can be achieved by feeding a force signal.

An electric-pneumatic (EP) regulator with a resolution of 0.5 kPa is integrated into the HPK_o simulator to automatically control the pore pressure. A feedback control loop is used to adjust regulators for specific stress paths. For pore water pressure, the regulated air pressure is applied to an air/fluid pressure converter that turns the pneumatic pressure to water pressure. The water pressure is connected to an electric volume change indicator before it is directed to the bottom drainage of the specimen.

3.5 Testing Procedure

The testing procedure is divided into three phases; including specimen saturation, K_o consolidation, and application of pore pressure variations. Moisture tamping was used to prepare uniform specimens without particle segregation. The majority of air was expelled from the specimen by water flushing from bottom to top under a 5 kPa pressure difference. After this, vertical pressure and back pressure were applied simultaneously with a stress increment of 5 kPa for 3 minutes to reach stress equilibrium. When the back pressure reached 110 kPa, the stress components held for saturation. A B-value check in K_o condition (Chang *et al.* 2014) was performed, and a B-value greater than 0.95 is needed for saturation. Additionally, compression wave velocity (V_p) measurement using bender elements was also conducted in the developing stage, and a V_p value greater than 1500 m/s was needed to ensure saturation (Allen *et al.* 1980).

After the completion of saturation, K_o consolidation was performed using a vertical stress increment of 5 kPa to the effective vertical consolidation stress while maintaining the back pressure of 110 kPa. The completion of K_o consolidation was determined based on two criteria: (1) the excess pore pressure at bottom reducing to zero, and (2) no volume change recorded for 5 minutes. Additionally, the dissipation durations for different stress levels were also recorded. An effective vertical consolidation stress of 200 kPa was used to prepare K_o-consolidated specimens for sinusoidal pore pressure variations.

After the completion of K_o consolidation, sinusoidal pore pressure variations were slowly applied while maintaining constant vertical stress. A multi-stage testing procedure was adopted to apply repeated loadings. For each pore pressure amplitude, the pore pressure was slowly ramped to the target value over a set period based on K_o consolidation results. Theoretically, the period of a complete cycle of pore pressure variation is four times the dissipation time in monotonic loading. To ensure full dissipation during the cyclic loading, six times of the dissipation time in monotonic loading was used for a ramping period. The suitability of this ramping period was checked from the pore pressure measurements at the bottom drainage.

The pore pressure variation procedure was programed using a computer-based controller and DAQ to automatically perform the BPCC. The repeated loading stage stopped when the induced increment of permanent vertical displacement of five consecutive cycles was constant and the next loading amplitude was performed after the data were saved. The testing results show that the system meets the design requirements and the procedure is adequate.

4. TEST RESULTS

4.1 Properties of Samples and Testing Program

Remolded specimens of Ottawa sand mixed with 0%, 10%, and 20% of mica contents (MC) in weight were tested in this study. The mica powder is added with Ottawa sand because mica content is the key factor to induce high compressibility of granular soils in central-western Taiwan (Huang *et al.* 1999). The physical properties of the soils are listed in Table 1, and the grain size distribution curves of all specimens along with the pure mica powder are shown in Fig. 2. Moist tamping with 5% water content in three layers was used to prepare remolded specimens with or without mica. The Ottawa sand is uniform sand (USCS classification of SP) from Ottawa, USA with mean grain size (D_{50}) of 0.65 mm, and primarily comprises quartz with a specific gravity of 2.65. The maximum and minimum void ratios of the sand determined by the ASTM-D2049 method are 0.75 and 0.48, respectively. The one-dimensional compression curve of clean Ottawa sand is conducted using the HPK_o simulator subjected to increasing vertical stress, and the results are shown in Fig. 3. The mica content is a low plasticity powder from a commercial supplier of painting additives. The USCS classification of the mica powder is CL-ML, with a mean grain size of 0.013 mm. The sand specimens with mica contents of 10 and 20% are classified as SC-SM in USCS classification system and were tested to investigate the effects of mica content on the compressibility of granular soils.

Based on previous studies on monotonic compression behaviors, the compressibility of granular soils is mainly affected by the initial state, stress level, and soil composition. The initial state is represented by the combination of vertical effective stress, void ratio, and OCR. To investigate factors affecting the shakedown responses of saturated granular soils subjected to repeated pore pressure variations, a testing program including three mica contents for two K_o consolidated void ratios was conducted. All the loose specimens (*i.e.,* higher void ratio) of the same fines content were prepared at the same void ratio by moist tamping with 5% water content. The loose specimens were then applied 200 kPa vertical effective stress and the after-consolidated void ratios are reported in Table 2. These specimens are in the the normally consolidated state. The dense specimens are the same specimen after the completion of applying sinusoidal loadings. The minimum loading cycles required to reach a shakedown state is defined as the shakedown cycle (N_{SD}). The testing program is listed in Table 2, and the N_{SD} values for different amplitudes are also presented.

Table 1 Physical properties of testing soils

Physical properties	Ottawa sand	Mica
D_{60} (mm)	0.669	0.018
D_{50} (mm)	0.650	0.013
D_{30} (mm)	0.391	0.011
D_{10} (mm)	0.223	0.004
Coef. of uniformity, C_u	1.5	4.5
Specific gravity, G_s	2.65	2.85
LL (%)	–	34
PL (%)	–	27
PI (%)	–	7
USCS Classification	SP	CL-ML
e_{max}	0.75	–
e_{min}	0.48	–

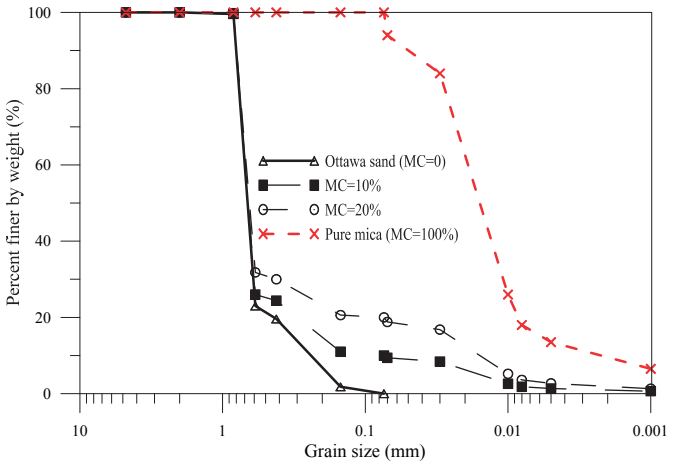

Fig. 2 Grain size distributions of testing soils

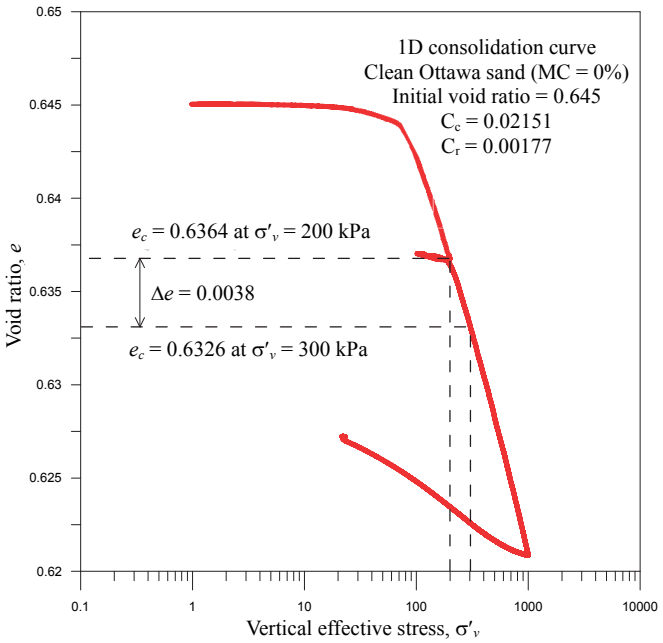

Fig. 3 One-dimensional compression curve of clean Ottawa sand

Table 2 Testing program and results

Mica content (%)	Consolidated void ratio e_c	Δu = 10 kPa N_{SD}	Δu = 25 kPa N_{SD}	Δu = 50 kPa N_{SD}	Δu = 75 kPa N_{SD}	Δu = 100 kPa N_{SD}
0	0.599	12	23	40	52	70
0	0.651	44	55	87	103	150
10	0.533	9	15	27	36	60
10	0.552	24	30	58	70	110
20	0.394	9	15	21	30	44
20	0.428	33	41	65	80	120

4.2 Results of Sinusoidal Loading

To perform multi-stage testing on a specimen, pore pressure amplitudes were gradually increased from 10 kPa to 100 kPa. The axial strain is calculated from the vertical displacement divided by the height of the specimen before the application of sinusoidal loading. The repeated loading results for clean Ottawa sand (MC = 0%) with consolidated void ratio (denoted as e_c) of 0.651 under vertical effective stress of 200 kPa are shown in Fig. 4. The time histories of pore pressure and axial strain along with the vertical effective stress-axial strain curves are shown in Figs. 4(a) ~ 4(c), respectively. Figure 4(a) shows the stress control performance of the simulator and variations of pore pressure amplitudes. Figure 4(b) shows that the permanent axial strain accumulates as the loading cycle increases under a constant loading amplitude. The hysteretic loops between the vertical effective stress and axial strain are shown in Fig. 4(c). The increment of plastic strain decreases as the loading cycle increases.

The results for Ottawa sand with 20% of mica content (MC = 20%), consolidated void ratio of 0.428 under vertical effective stress of 200 kPa are shown in Fig. 5. Five pore pressure amplitudes, including 10, 25, 50, 75, and 100 kPa, were applied in sequence after K_o consolidation. The time histories of axial strain (Fig. 5(b)) and the stress-strain curves (Fig. 5(c)) of the specimens with 20% mica show similar responses to those of clean sand, although with a larger axial strain. It shall be noted that the multi-stage testing procedure produces less consistent results because the accumulated void ratio reduction is more significant resulting in a different initial state. More detailed discussions of these features will be presented later.

4.3 Shakedown Behavior of Saturated Sands

The plastic strain magnitudes and loading cycles required to reach plastic shakedown state are two important features in the shakedown theorem. The definitions of the accumulative plastic strain and plastic strain increment are shown in Fig. 6(a), along with the hysteric loops for clean Ottawa sand subjected to a pore pressure amplitude of 100 kPa. The accumulative plastic strain after N cycles, denoted as $\varepsilon_{p,N}$ is defined as the plastic strain induced from the beginning of this loading stage. The plastic strain increment in the N^{th} cycle, denoted as $\Delta\varepsilon_{p,N}$ is defined as the induced plastic strain in this cycle. All strains are calculated using the specimen height before the application of the sinusoidal pore pressure variation in each loading stage. The two plastic strains are related as follows:

$$\varepsilon_{p,N} = \sum_{i=1}^{N} \Delta\varepsilon_{p,i} \tag{6}$$

Again, shakedown states with a zero or small plastic strain increment are referred to as plastic shakedown and plastic creep, respectively.

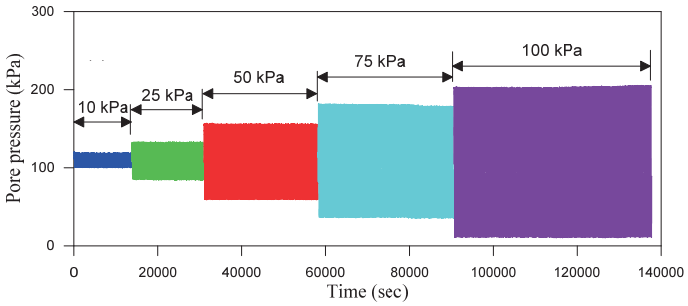

(a) Pore pressure

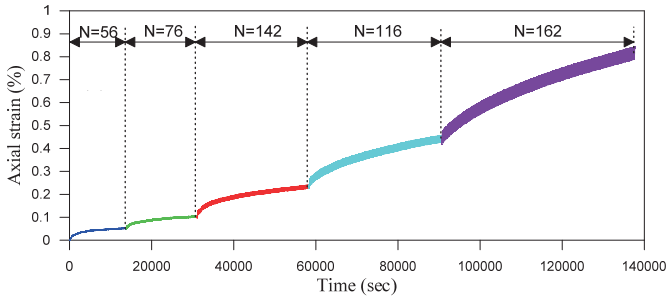

(b) Axial strain

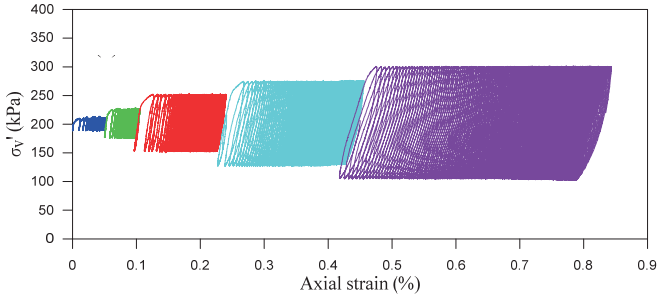

(c) Stress-strain curves

Fig. 4 Results of sinusoidal loading for MC = 0% and e_c = 0.651

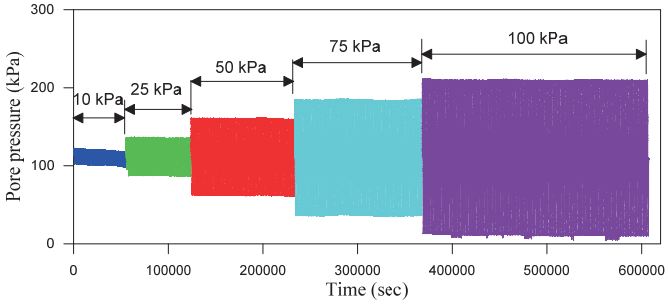

(a) Pore pressure

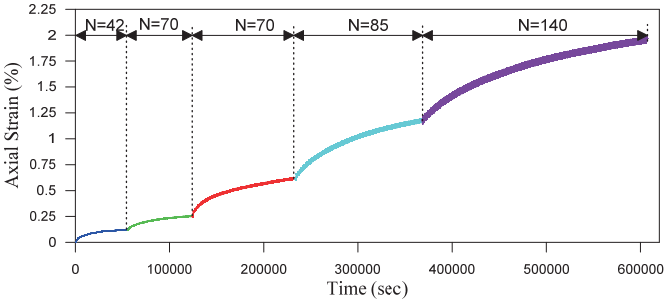

(b) Axial strain

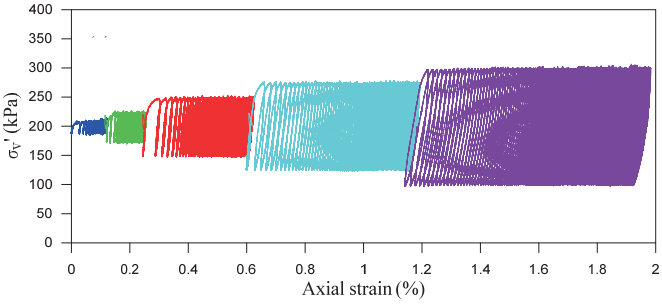

(c) Stress-strain curves

Fig. 5 Results of sinusoidal loading for MC = 20% and e_c = 0.428

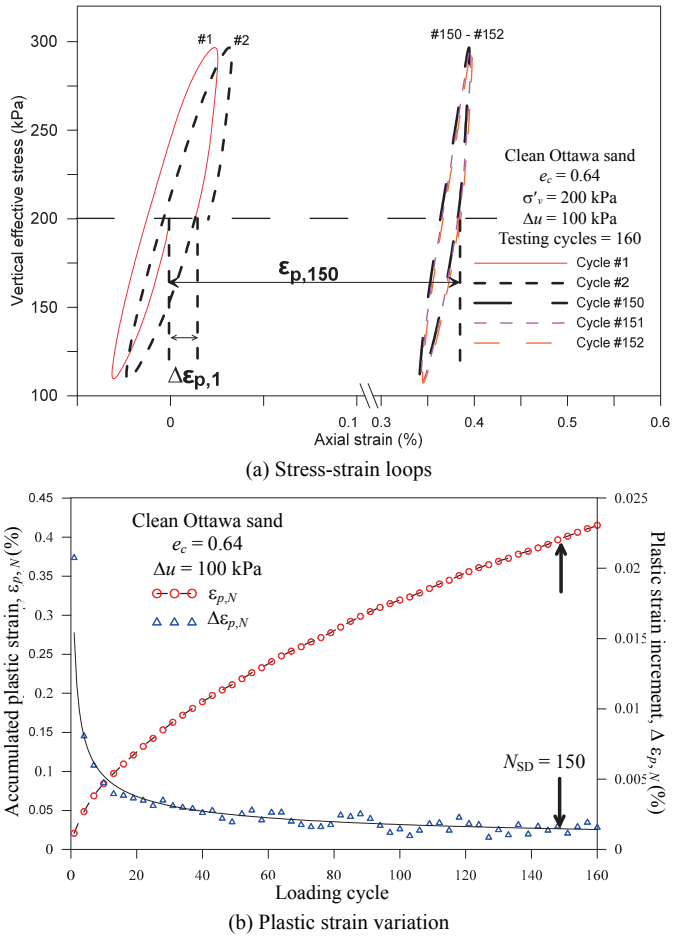

Fig. 6 Determination of plastic shakedown state

To determine the initiation of the plastic shakedown state, the variation of plastic strain increment is plotted with the corresponding accumulative plastic strain curve, as shown in Fig. 6(b). The plastic strain increment reached a stable and small value after the 150th cycle, and the accumulative plastic strain curve shows a linear relationship with loading cycles. The N_{SD} for this loading amplitude is 150. The hysteric loops in Fig. 6(a) also show the resilient behavior of shaken down soil, and the nonlinear hysteric response in the shakedown state revealed that the granular specimen is in a plastic shakedown state.

Following this procedure, the plastic strain increment curves of the specimen with MC = 20% and e_c = 0.428 are shown in Fig. 7, in which the N_{SD} for each loading amplitude is indicated by an arrowhead. The accumulative strain curves of three specimens with various mica contents are shown in Fig. 8 along with the marked N_{SD}. The curves in Fig. 8 (c) are calculated from Fig. 7 using Eq. (6). The results show that a plastic shakedown behavior occurs at small loading amplitudes and the plastic creep response exists for loading amplitudes exceeding a certain level (*e.g.,* 50 kPa in Fig. 7). Nevertheless, the results show that K_o compression is always below the plastic shakedown limits for all the testing conditions.

4.4 Factors Affecting the Shakedown Behavior of Saturated Sands

To show the significance of compressibility from the shakedown effect, the ratio of the accumulative plastic strain at the initiation of plastic shakedown ($\varepsilon_{p,ps}$) to the plastic strain induced in the first cycle ($\varepsilon_{p,1}$), which is considered in conventional consolidation theory, is defined as shakedown compression ratio (SCR) (Chang *et al.* 2017), which is expressed as:

$$\mathrm{SCR} = \frac{\varepsilon_{p,ps}}{\varepsilon_{p,1}} \tag{7}$$

where $\varepsilon_{p,ps}$ is calculated from the accumulative axial strain at the N_{SD} cycle. The $\varepsilon_{p,1}$ is the plastic axial strain induced in the first loading cycle. The SCR represents the increasing ratio of accumulative plastic strain from repeated loadings.

Variations between the pore pressure amplitudes (Δu), accumulative plastic strains at the initiation of plastic shakedown ($\varepsilon_{p,ps}$), and N_{SD} values are shown in Fig. 9. Figure 9(a) reveals that the $\varepsilon_{p,ps}$ increases as the pore pressure amplitude rise and soils with a higher void ratio also induced a higher $\varepsilon_{p,ps}$ value. The small difference of $\varepsilon_{p,ps}$ between the 10 and 20 kPa of pore pressure amplitudes is attributed to the exceedance of the void ratio effect from previous repeated loading over the current loading amplitude. Figure 9(b) shows that the N_{SD} value increases linearly with Δu and initially loose soils require more cycles to reach the plastic shakedown state.

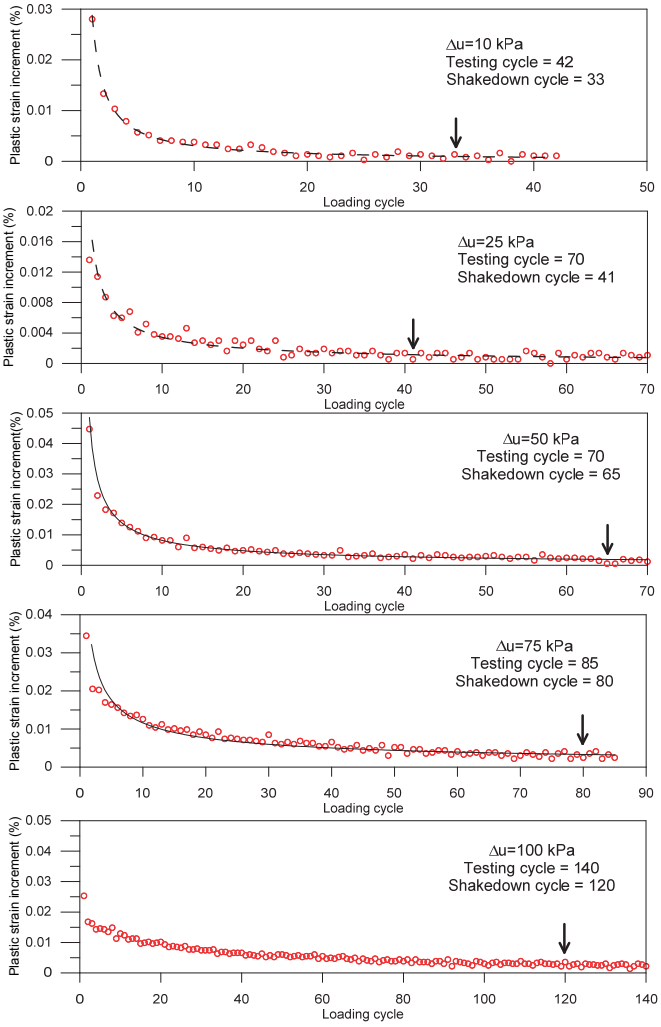

Fig. 7 Plastic strain increment of the specimen with MC = 20% and e_c = 0.428

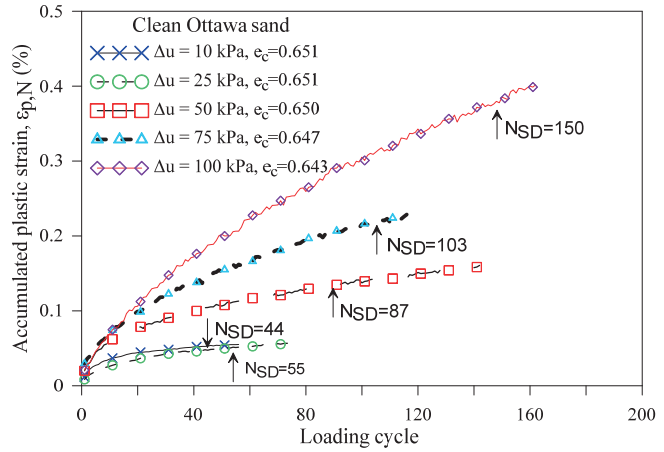

(a) MC = 0%, e_c = 0.651

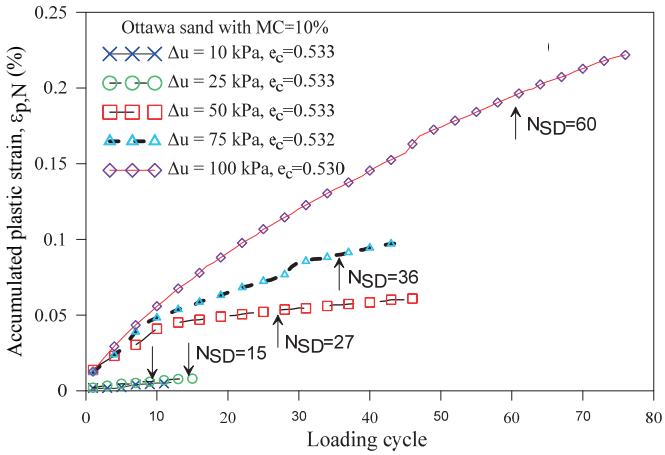

(b) MC = 10%, e_c = 0.533

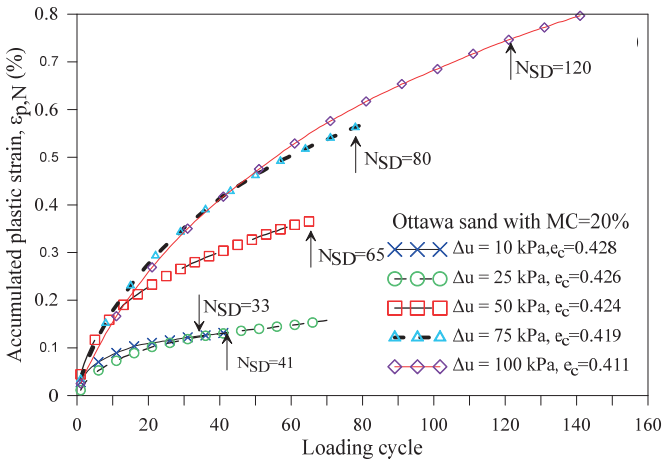

(c) MC=20%, e_c = 0.428

Fig. 8 Accumulated plastic strain curves

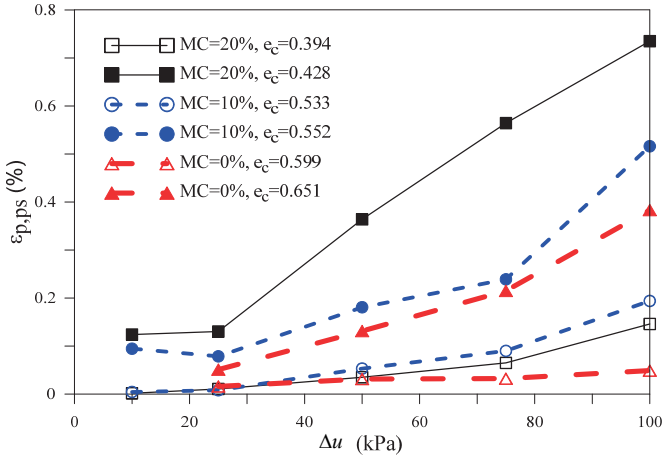

(a) Accumulative plastic strain

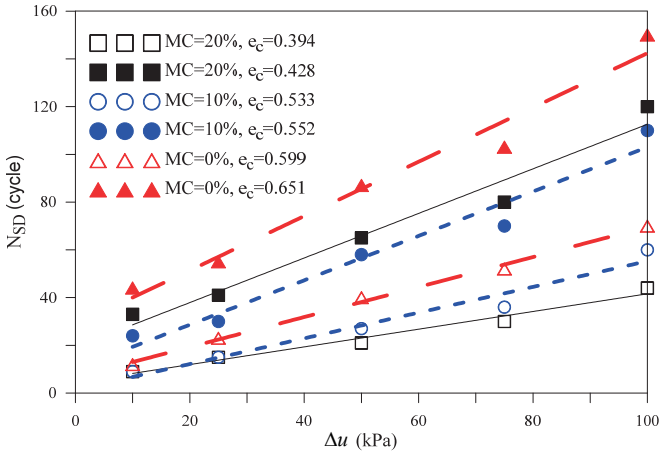

(b) Cycles to shakedown initiation

Fig. 9 Effect of pore pressure amplitude on shakedown responses

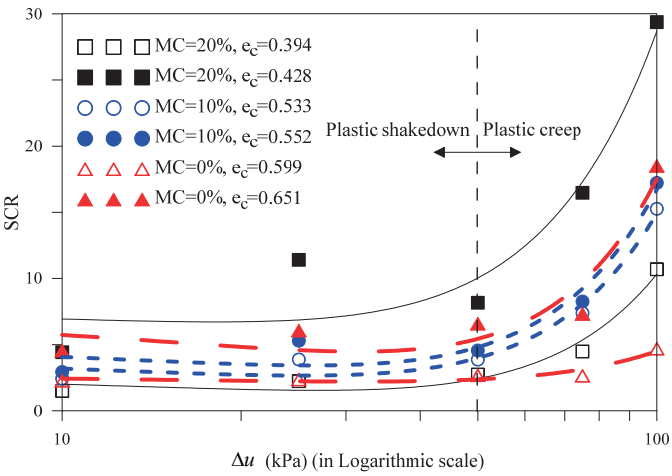

Fig. 10 Effects of repeated loading on compression of granular soils

Figure 10 shows the variation of SCR with pore pressure amplitude for all specimens. Although nonlinear relationships exist between the SCR and Δu, an approximate constant SCR was observed for Δu less than 50 kPa, which is also the boundary value dividing plastic shakedown and plastic creep, as shown in Figs. 7 and 8. This feature is important for predicting and controlling the compression of granular soils subjected to pore pressure fluctuations. Additionally, the results also reveal that the SCR values of plastic creep could be up to 29.4 times for sand with mica, and 18.5 times for clean sand. The SCR values of plastic shakedown (*i.e.*, Δu no greater than 50 kPa) are reduced to 8.2 times for sand with mica and 6.6 times for clean sand. These values provide the basis for explaining the field subsidence monitoring data, and evidently reveal the significance of shakedown compression in ground subsidence with thick aquifer layers.

4.5 Comparison of Monotonic and Shakedown Compression

To implement the shakedown compression in ground subsidence analysis, the compression of an aquifer layer, which is consisted of saturated, granular soils, is divided into two components: the monotonic compression from the long-term pore pressure trend and shakedown compression from pore pressure fluctuations. The first part can be estimated from conventional consolidation theory for settlement estimation. For normally consolidated soil, the volumetric strain (ε_v) is calculated by:

$$\varepsilon_v = \frac{C_c}{1+e_c}\log\left(\frac{\sigma'_{v,0}+\Delta\sigma'_v}{\sigma'_{v,0}}\right) \tag{8}$$

where C_c is the compression index, $\sigma'_{v,0}$ is the initial vertical effective stress, and $\Delta\sigma'_v$ is the increase in vertical effective stress.

To compare the compression components from monotonic and repeated loading, a monotonic compression test is performed on clean remolded Ottawa sand with a preconsolidation stress of 200 kPa and the void ratio is close to the initial value of repeated loading. The monotonic compression curve is overlapped with the repeated loading data of pore pressure amplitude of 100 kPa as shown in Fig. 11, in which the variation of the void ratio is used to reduce the difference in the initial void ratio. It should be noted that the repeated loading is from a multi-stage test, in which the preconsolidation stress was 275 kPa before the application of sinusoidal amplitude of 100 kPa, while the preconsolidation stress in the monotonic compression curve is 200 kPa. The permanent deformation in the first cycle corresponds to the compression from 275 to 300 kPa. Therefore, the repeated loading result is mainly from the shakedown effect, and the repeated loading compression is 2.3 times the monotonic value for this stress condition.

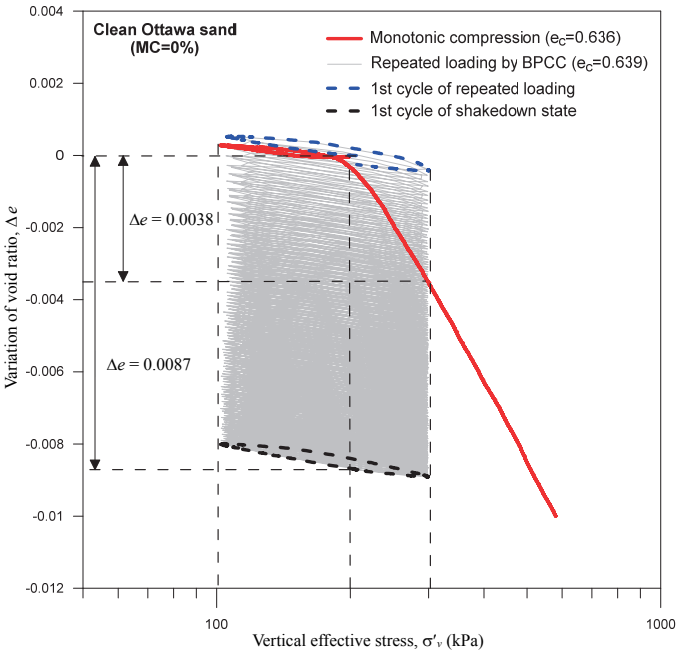

Fig. 11 Compression curves from monotonic and repeated loadings

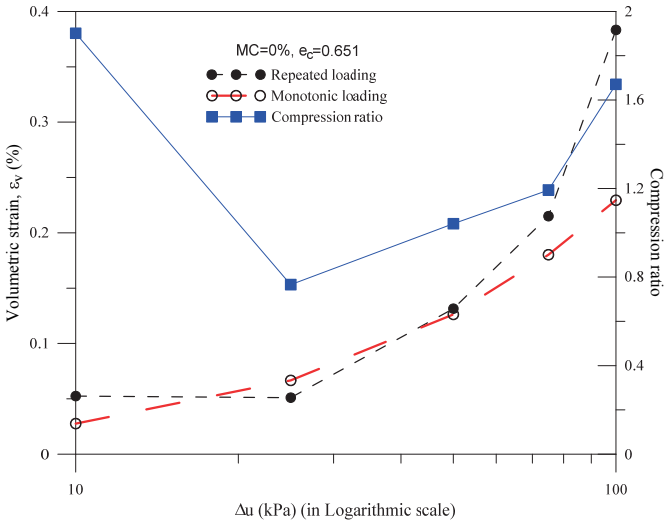

Fig. 12 Comparison of compression from monotonic and repeated loadings

To compare the monotonic and shakedown compression components of granular soils at specific void ratios, the volumetric strains calculated from Eq. (8) referring to $\sigma'_{v,0}$ of 200 kPa and C_c value of 0.0215 are plotted in Fig. 12, along with the shakedown volumetric strains for the same pore pressure amplitudes. The ratios between the monotonic and shakedown volumetric strains are also shown in the same plot. This comparison shows that the shakedown compression is at least as significant as the monotonic component for plastic shakedown cases and the shakedown effect should be included in ground subsidence analysis.

5. SUMMARY AND CONCLUSION

Long-term field monitoring data revealed that soil compression in aquifer layers could be a significant source of ground subsidence and conventional consolidation theory is incapable of describing the temporal variations in subsidence. Compression of saturated, granular soils due to pore pressure fluctuations might be the missing part of the puzzle here. To investigate the mechanism of granular soil compression due to repeated pore pressure variations, a modified Rowe cell is developed to apply a stress path that simulates the pore pressure fluctuations while maintaining constant vertical stress. The system is called the *HPK*$_0$ simulator, and the testing procedure is termed back-pressure-control consolidation (BPCC). The shakedown theorem is extended to saturated, granular soils under K_o condition. Remolded sand specimens with different mica contents and void ratios were tested to study the shakedown behaviors. The major findings are listed as follows:

1. The testing results reveal that the shakedown theorem can be applied on saturated, granular soils under K_o condition. Experimental results show that saturated granular soils under K_o condition will be below the plastic shakedown limit and reach a plastic shakedown state that shows a resilient response with a zero or small but constant plastic strain increment.
2. The major factors that affect the shakedown responses are the loading (pore pressure) amplitude, soil composition (mica content), and initial state. The loading amplitude affects the accumulative plastic strain at shakedown state, the number of cycles to initiate plastic shakedown state, and the type of

resilience, including plastic shakedown and plastic creep. The plastic strain at plastic shakedown increases with an increase in mica content and initial void ratio. The number of cycles to initiate plastic shakedown increases along with the loading amplitude and initial void ratio.

3. A comparison of the SCR values, which represent the increase in the accumulative plastic strain from repeated loadings, shows that a relatively constant SCR was observed for pore pressure amplitudes less than the boundary value dividing plastic shakedown and plastic creep. The SCR value increases with increasing mica content and initial void ratio.
4. Comparisons of monotonic and shakedown compressions reveal that the shakedown compression is at least as significant as the monotonic component for plastic shakedown cases, and thus that the shakedown effect should be included in ground subsidence analysis.

Based on the compression study of saturated, granular soils subjected to repeated loading carried out in this work, a tentative framework for ground subsidence prediction/analysis is proposed. The total compression is divided into long-term and fluctuating components. The compression due to a long-term reduction in pore pressure can be estimated using a monotonic compression curve. The fluctuation component can be estimated based on shakedown features, including the magnitude of plastic strain, plastic limit, and N_{SD}. Furthermore, the available discharge volume of the aquifer layer can be determined based on subsidence prediction and pore pressure control.

As the present paper is a pilot study in this issue, there are some limitations on current findings. First, the qualitative results are valid but the quantitative predictions for different soils shall be cautious as the data are mainly from artificial soils. Second, the loading sequences in the field will be different from sinusoidal types and the effects of loading sequence need further investigation. Those points are beyond the scope of current study and will be the next step to develop practical procedure for field applications.

ACKNOWLEDGEMENTS

This study was supported by the Ministry of Science and Technology, Taiwan, under grants NSC 102-2119-M-009-001 and MOST 106-2221-E-006-072-MY2, which are gratefully acknowledged. Any opinions, findings, and conclusions or recommendations expressed in this material are those of the authors and do not necessarily reflect the views of the Ministry of Science and Technology, Taiwan.

NOTATIONS

C_c	Compression index
ε_v	Volumetric strain
Δu	Pore pressure amplitude (kPa)
e_c	Consolidated void ratio
$\varepsilon_{p,N}$	Accumulative plastic strain after N cycles
$\Delta\varepsilon_{p,N}$	Plastic strain increment in the N^{th} cycle
K_o	Coefficient of earth pressure at rest
MC	Mica content
N	Number of loading cycles
SCR	Shakedown compression ratio
σ'_v	Vertical effective stress (kPa)

REFERENCES

Allen, N.F., Richart, F.E., Jr., and Woods, R.D. (1980). "Fluid wave propagation in saturated and nearly saturated sands." *Journal of Geotechnical Engineering*, ASCE, **106**(3), 235-254. https://doi.org/10.1016/0148-9062(80)90593-8

Barksdale, R.D. (1972). "Laboratory evaluation of rutting in base course materials." *Proceedings of the 3rd International Conference on Structural Destruction of Asphalt Pavements*, 161-174.

Biot, M.A. (1941). "General theory of three-dimensional consolidation." *Journal of Applied Physics*, **12**(2), 155-164. https://doi.org/10.1063/1.1712886

Burbey, T.J. (2006). "Three-dimensional deformation and strain induced by municipal pumping, Part 2: Numerical analysis." *Journal of Hydrology*, **330**(3), 422-434. https://doi.org/10.1016/j.jhydrol.2006.03.035

Casagrande, A. (1960). *From Theory to Practice in Soil Mechanics*. Wiley and Sons, New York, U.S.A.

Chang, W.J., Chang, C.W., and Zeng, J.K. (2014). "Liquefaction characteristics of gap-graded gravelly soils in K_o condition." *Soil Dynamics and Earthquake Engineering*, **56**, 74-85. https://doi.org/10.1016/j.soildyn.2013.10.005

Chang, W.J., Chou, S.H., and Huang, A.B. (2017). "Physical simulation of aquifer compression due to groundwater fluctuation." *Engineering Geology*, **231**, 157-164. https://doi.org/10.1016/j.enggeo.2017.10.012

Chuhan, F.A., Kjeldstad, A., Bjørlykke, K., and Høeg, K. (2003). "Experimental compression of loose sands: Relevance to porosity reduction during burial in sedimentary basins." *Canadian Geotechnical Journal*, **40**(5), 995-1011. https://doi.org/10.1139/t03-050

Hill, M.C., Banta, E.R., Harbaugh, A.W., and Anderman, E.R. (2000). *MODFLOW-2000, The U.S. Geological Survey Modular Ground-Water Model. U.S. Geological Survey Open-File*, Report 00-184.

Huang, A.B., Hsu, S.P., and Kuhn, H.R. (1994). "A multiple purpose soil testing apparatus." *Geotechnical Testing Journal*, **17**(2), 227-232. https://doi.org/10.1520/GTJ10094J

Hung, W.C., Hwang, C., Liou, J.C., Lin, Y.S., and Yang, H.L. (2012). "Modeling aquifer-system compaction and predicting land subsidence in central Taiwan." *Engineering Geology*, 147-148, 78-90. https://doi.org/10.1016/j.enggeo.2012.07.018

Koiter, W.T. (1960). "General theorems for elastic-plastic solids." *In Progress in Solid Mechanics*. I. Sneddon and R. Hill, Eds., 165-221.

Lambe, T.W. and Whitman, R.V. (1969). *Soil Mechanics*. Wiley, New York, U.S.A.

Lee, K. (1981). "Consolidation with constant rate of deformation." *Geotechnique*, **31**(2), 215-229. https://doi.org/10.1680/geot.1981.31.2.215

Leshchinsky, D. and Rawlings, D.L. (1988). "Stress path and permanent deformations in sand subjected to repeated load." *Geotechnical Testing Journal*, ASTM, **11**(1), 36-43. https://doi.org/10.1520/GTJ10642J

Melan, E. (1938). "Der spannungsgudstand eines Henky-Mises schen Kontinuums bei Verlandicher." elastung. *Sitzungberichte der Ak Wissenschaften Wie* (Ser. 2A), 147-173.

Nakata, Y., Hyodo, M., Hyde, A.F.L., Kato, Y., and Murata, H. (2001). "Microscopic particle crushing of sand subjected to high pressure one-dimensional compression." *Soils and Foundations*, **41**(1), 69-82. https://doi.org/10.3208/sandf.41.69

Pestana, J.M. and Whittle, A.J. (1995). "Compression model for cohesionless soils." *Geotechnique*, **45**(4), 611-631. https://doi.org/10.1680/geot.1995.45.4.611

Terzaghi, K. (1925). *Principles of Soil Mechanics*. McGraw-Hill, New York, U.S.A.

Rowe, P.W. and Barden, L. (1966). "A new consolidation cell." *Geotechnique*, **16**(2), 519-539. https://doi.org/10.1680/geot.1966.16.2.162

Werkmeister, S., Dawson, A., and Wellner, F. (2004). "Pavement design model for unbound granular materials." *Journal of Transportation Engineering*, ASCE, **130**, 665-674. https://doi.org/10.1061/(ASCE)0733-947X(2004)130:5(665)

Wissa, A.E.Z., Christian, J.T., Davis, E.H., and Heiberg, S. (1971). "Consolidation at constant rate of strain." *Journal of the Soil Mechanics and Foundations Division*, ASCE, **97**(1), 1393-1413.

Yu, H.S. (2005). "Three-dimensional analytical solutions for shakedown of cohesive-frictional materials under moving surface loads." *Proceedings of Royal Society A*, **461**, 1951-1964. https://doi.org/10.1098/rspa.2005.1445